ADVANCED ELECTRONIC MATERIALS
www.advelectronicmat.de

Weavable, High-Performance, Solid-State Supercapacitors Based on Hybrid Fibers Made of Sandwiched Structure of MWCNT/rGO/MWCNT

Gengzhi Sun, Xiao Zhang, Rongzhou Lin, Bo Chen, Lianxi Zheng, Xiao Huang, Ling Huang, Wei Huang, Hua Zhang,* and Peng Chen**

The emergence of weavable electronics urgently calls for the development of compatible energy storage devices that can be woven into textiles. Due to their high power density, fast charge–discharge rate and long cycling lifetime, fiber-based supercapacitors are attracting particularly increasing interest.[1] Although some fiber-based supercapacitors have been reported,[2–7] it still remains a challenge to ensure both high capacitive performance and good weavability/knittability.

Graphene and carbon nanotubes (CNTs) are promising carbon materials to construct fiber electrodes because of their high electrical and thermal conductivities, mechanical strength and flexibility, large specific surface area, and amenability to be spun into fibers.[1] For example, long conductive fibers made of reduced graphene oxide (rGO) have been prepared by using the wet spinning method,[8–13] but these rGO fibers are fragile.[8,9] In addition, due to the irregular assembly of rGO nanosheets in the rGO fibers, their poor mechanical property arising from the internal abrasion and stress concentration cannot be avoided.[12,13]

Dr. G. Z. Sun, Prof. X. Huang,
Prof. L. Huang, Prof. W. Huang
Key Laboratory of Flexible Electronics (KLOFE)
& Institute of Advanced Materials (IAM)
Jiangsu National Synergetic Innovation
Center for Advanced Materials (SICAM)
Nanjing Tech University (NanjingTech)
30 South Puzhu Road, Nanjing 211816, China
E-mail: iamlhuang@njtech.edu.cn
Dr. G. Z. Sun, Prof. P. Chen
School of Chemical and Biomedical Engineering
Nanyang Technological University
70 Nanyang Drive, Singapore 637457, Singapore
E-mail: chenpeng@ntu.edu.sg
X. Zhang, B. Chen, Prof. H. Zhang
Center for Programmable Materials
School of Materials Science and Engineering
Nanyang Technological University
50 Nanyang Avenue, Singapore 639798, Singapore
E-mail: HZhang@ntu.edu.sg
R. Z. Lin
School of Mechanical and Aerospace Engineering
Nanyang Technological University
50 Nanyang Avenue, Singapore 639798, Singapore
Prof. L. X. Zheng
Department of Mechanical Engineering
Khalifa University of Science
Technology, and Research
Abu Dhabi 127788, United Arab Emirates

DOI: 10.1002/aelm.201600102

Although the rGO nanosheet is expected to exhibit high capacitance due to its large specific surface area and pseudocapacitance arising from the existence of abundant of oxygen-containing functional groups,[14] its restacking and poor conductivity seriously deteriorate the capacitive performance of the formed rGO fiber, especially at high current density.[15] As known, CNT fibers usually exhibit good flexibility, excellent electrical conductivity, and high mechanical strength,[16–20] but the low intrinsic capacitance of CNTs hinders their application in supercapacitors.[21] Hence, the combination of rGO nanosheets and CNTs may provide a better way for preparation of fiber-based supercapacitors with improved performance,[15,22,23] since the incorporated CNTs not only can greatly prevent the restacking of rGO nanosheets and thus increase the electrolyte accessible surface area, but also can provide the highly electrical conductive pathway. However, in the previous work,[15,22,23] the surfactants and strong oxidants are normally used in order to achieve well-dispersed suspension of CNTs with short length (0.5–3 μm) and GO nanosheets. Therefore, it unavoidably compromised the electrical and mechanical properties of the resulting hybrid CNT-rGO fibers.[22,23] In addition, the randomly dispersed mixture of CNTs and rGO nanosheets in CNT-rGO fibers may not be ideal to maximize their synergistic effect to improve the capacitive performance. Recently, the laminated structures with alternating CNT and rGO layers were fabricated, which exhibited better mechanical, electrical, and electrochemical properties.[24,25] In addition, the orientation of incorporated CNTs is also important to determine the mechanical strength and electrical conductivity of the resultant hybrid CNT-rGO fibers.[26]

In this Communication, we report a method to fabricate highly flexible hybrid fibers with a sandwiched structure, i.e., multi-walled CNT (MWCNT)/rGO/MWCNT, which was formed by incorporation of well-aligned and long MWCNTs and rGO nanosheets. Importantly, the non-involvement of surfactants, oxidative treatments, and any other harsh chemical processes result in the excellent mechanical, electrical, and electrochemical properties of MWCNT/rGO/MWCNT fibers. As a proof-of-concept application, these hybrid fibers are used to construct solid-state supercapacitors, which exhibit excellent weavability, high volumetric capacitance and energy density, and good cycling stability.

As schematically shown in **Figure 1**a, after a continuous and well-aligned MWCNT sheet (≈1.5 mm × 8.5 cm) was pulled out from a vertical array of MWCNTs with height of ≈400 μm (Figure S1, Supporting Information), two layers of MWCNT sheets were stacked onto a polytetrafluoroethylene

ADVANCED ELECTRONIC MATERIALS
www.advelectronicmat.de

www.MaterialsViews.com

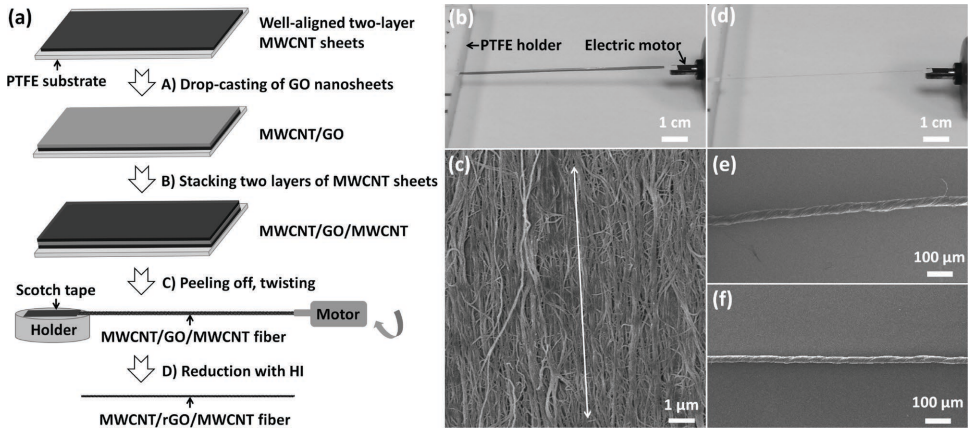

Figure 1. a) Schematic illustration of fabrication of MWCNT/rGO/MWCNT fibers. b) Photograph of a MWCNT/GO/MWCNT film. c) SEM image of the aligned MWCNTs on the surface of MWCNT/GO/MWCNT film. The arrow indicates the alignment of MWCNTs. d) Photograph of a twisted MWCNT/GO/MWCNT fiber. e) SEM image of a MWCNT/GO/MWCNT fiber. f) SEM image of a MWCNT/rGO/MWCNT fiber.

(PTFE) substrate.[27] After the single-layered GO nanosheets (Figure S2, Supporting Information) dispersed in dimethylformamide (DMF) were drop-casted onto the two-layer MWCNT sheets (Step A in Figure 1a), referred to as MWCNT/GO, and dried in a fume hood at room temperature, another two-layer MWCNT sheets were laid on the top of MWCNT/GO to form a sandwiched hybrid film (Step B in Figure 1a), referred to as MWCNT/GO/MWCNT. The obtained film was peeled off from the PTFE substrate and then twisted into a fiber by using a motor with a rotation rate of 200 rpm for 2 min (Step C in Figure 1a), which is similar to the process of Archimedean twist reported previously.[27,28] Finally, the MWCNT/GO/MWCNT fiber was chemically reduced by hydriodic acid (HI) to obtain the MWCNT/rGO/MWCNT fiber (Step D in Figure 1a).[27] Figure 1b shows the photograph of a MWCNT/GO/MWCNT film suspending between a PTFE holder and an electric motor. The scanning electron microscopy (SEM) image suggests that the MWCNTs on the surface of MWCNT/GO/MWCNT film were orientated in the same direction (Figure 1c). After twisting (Figure 1d), the MWCNT/GO/MWCNT fiber with diameter of ≈40 μm was obtained (Figure 1e and Figure S3a, Supporting Information), which was then chemically reduced with HI.[29] The resulting MWCNT/rGO/MWCNT fiber became more packed and its diameter decreased to ≈30 μm (Figure 1f and Figure S3b, Supporting Information), due to removal of the oxygenated functional groups on GO nanosheets and the intercalated water molecules between GO nanosheets.[11] As shown in the X-ray photoelectron spectroscopy (XPS) C1s spectra (Figure S4, Supporting Information), after the reduction of GO nanosheets with HI, the relative intensity of C—O and C=O peaks at 286.3 and 288.0 eV, respectively, were greatly reduced, confirming the removal of oxygenated functional groups on GO nanosheets.[30]

Compared to the bare MWCNT fiber with conductivity of ≈380 S cm^{-1}, the conductivity of MWCNT/rGO/MWCNT fiber was compromised by the incorporation of rGO nanosheets and decreased with the original loading amount of GO nanosheets (**Figure 2**a). As a proof-of-concept application, a solid-state supercapacitor was fabricated using a pair of MWCNT/rGO/MWCNT fibers with space of ≈0.5 mm coated with polyvinyl alcohol (PVA)-H_2SO_4 gel on a glass substrate (inset of Figure 2b). The specific volumetric capacitance (C_V) was calculated from the discharge curve at current density of 1.0 A cm^{-3} (Figure S5, Supporting Information). As shown in

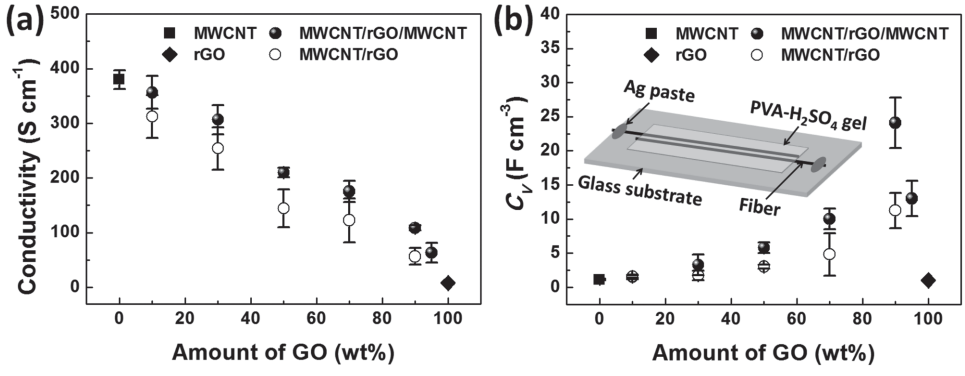

Figure 2. a) The conductivities of MWCNT, rGO, MWCNT/rGO/MWCNT, and MWCNT/rGO fibers as a function of the loading amount of GO nanosheets (wt%). b) The volumetric capacitances (C_V) of solid-state supercapacitors made of MWCNT, rGO, MWCNT/rGO/MWCNT, or MWCNT/rGO fibers as a function of the loading amount of GO (wt%). Inset: The schematic structure of solid-state fiber-based supercapacitor on glass substrate. The average C_V and standard deviation (error bar) were obtained from the measurement of three samples.

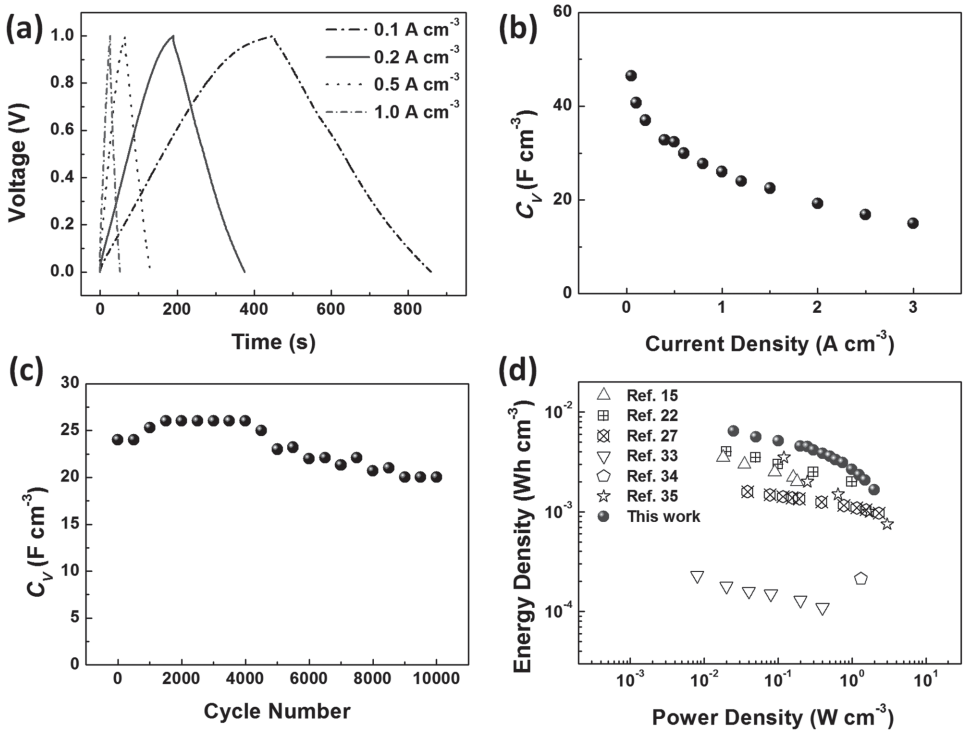

Figure 3. a) Galvanostatic charge–discharge curves of a MWCNT/rGO/MWCNT fiber-based supercapacitor (90 wt% of GO loading) at current density of 0.1, 0.2, 0.5, and 1.0 A cm^{-3}. b) The plot of C_V versus current density for a MWCNT/rGO/MWCNT fiber-based supercapacitor (90 wt% of GO loading). c) Cycling stability of a MWCNT/rGO/MWCNT fiber-based supercapacitor (90 wt% of GO loading) at the current density of 1.0 A cm^{-3}. d) Ragone plots of our fiber-based supercapacitor (90 wt% of GO loading) and other previously reported fiber-based supercapacitors.

Figure 2b, the maximum C_V of 24.1 ± 3.7 F cm^{-3} was obtained for the MWCNT/rGO/MWCNT fiber with 90 wt% of GO loading. At beginning, its C_V increased with the GO loading, while too much GO loading deteriorated the C_V due to the decreased conductivity of the MWCNT/rGO/MWCNT fiber, which was evidenced by the increased *IR* drop induced by the internal resistance of the supercapacitor (Figure S5, Supporting Information). Importantly, the C_V of MWCNT/rGO/MWCNT fiber-based supercapacitors is superior to the MWCNT/rGO fiber-based ones at the same GO loading, confirming the structural advantage of sandwiched MWCNT/rGO/MWCNT fibers.

In the following experiments, all the solid-state supercapacitors are fabricated based on the MWCNT/rGO/MWCNT fibers with GO loading of 90 wt%. **Figure 3**a depicts the galvanostatic charge–discharge curves of the MWCNT/rGO/MWCNT fiber-based supercapacitor at various charge–discharge current densities. The calculated C_V decreased from 40.7 F cm^{-3} at current density of 0.1 A cm^{-3} to 14.9 F cm^{-3} at current density of as high as 3.0 A cm^{-3} (Figure 3b). The measured C_V at 1.0 A cm^{-3} (26.1 F cm^{-3}) is higher than those of previously reported CNT-rGO fiber-based supercapacitors.[15,22,23] Furthermore, our hybrid fiber-based supercapacitor exhibits outstanding cycling stability. In particular, 83.3% of its capacity retained even after 10 000 cycles at the high current density of 1.0 A cm^{-3} (Figure 3c). The initial slight increase of C_V can be attributed to the activation of rGO nanosheets and the wetting of hybrid fibers.[31,32]

The energy density (*E*) and power density (*P*) were calculated based on $E = \frac{1}{2}CV^2$ and $P = E/t_{dis}$, respectively, where *C*, *V*, and t_{dis} are the capacitance, voltage range, and discharging time, respectively. The performance of our hybrid MWCNT/rGO/MWCNT fiber-based supercapacitors (90 wt% of GO loading) is compared with others reported previously (Figure 3d). At a given power density, the energy density of our supercapacitor is higher than those of others based on the MnO_2/carbon fibers,[33] MWCNT fibers,[34] porous MnO_2/MWCNT fibers,[35] and MoS_2-rGO/MWCNT fibers.[27] It is also superior to the recently reported solid-state supercapacitors based on the CNT-rGO fibers, which were fabricated using the wet spinning method[15] and silica capillary-based hydrothermal microreactor,[22] respectively.

Because of the facile fabrication method and unique fiber-shape structure, multiple devices can be easily connected in parallel to increase the overall capacity or in series to increase the output voltage in order to properly power the wearable electronics. As seen from the galvanostatic charge–discharge curves in **Figure 4**a, the charge storage capacity as indicated by the discharging time under a constant current was linearly proportional to the number of fiber-based supercapacitors connected in parallel. In addition, the voltage level, which can be reached at the given charging time and current, is linearly proportional to the number of fiber-based supercapacitors connected in series (Figure 4b). As a demonstration for practical application, a red light-emitting diode (LED) lightened by four fiber-based supercapacitors connected in series is shown in the inset in Figure 4b.

Importantly, the MWCNT/rGO/MWCNT fiber (90 wt% of GO loading) exhibited good flexibility. Similar to the bare

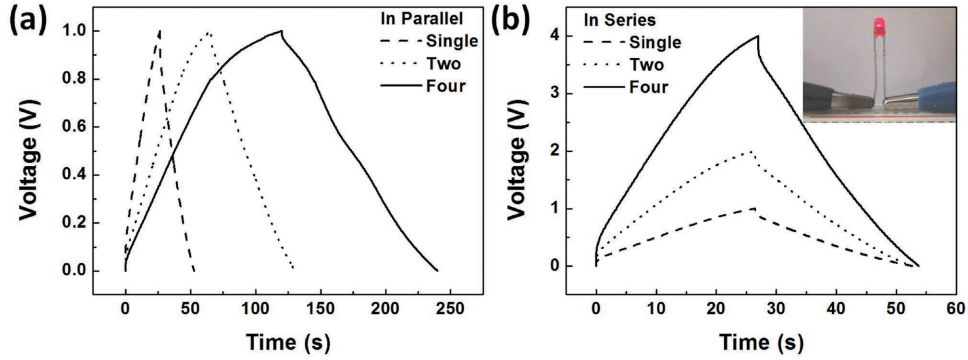

Figure 4. Galvanostatic charge–discharge curves of single, two, and four fiber-based supercapacitors (90 wt% of GO loading) connected in parallel a) at current density of 1.0 A cm^{-3}/the number of fiber-based supercapacitors or in series; b) at current density of 1.0 A cm^{-3}. Inset in (b): a red light-emitting diode is powered by a device with four fiber-based supercapacitors connected in series.

MWCNT fiber,[19] it can also be twisted into multi-ply fibers or tightly knotted (Figure S6, Supporting Information). In addition, its measured tensile strength, ≈110 MPa, is around three times higher than that of the cotton fiber.[36] All the aforementioned mechanical characteristics enable our hybrid fiber good weavability/knittability. Therefore, the solid-state supercapacitor based on MWCNT/rGO/MWCNT fibers (90 wt% of GO loading) has been woven into a fabric. Briefly, two MWCNT/rGO/MWCNT fibers (90 wt% of GO loading) were first sewn into a fabric in parallel using a steel needle (**Figure 5**a). Then a layer of PVA-H_2SO_4 gel was coated on the fabric surface. Due to the good flexibility and robustness of the hybrid fibers, the galvanostatic charge–discharge curves of the solid-state supercapacitor woven into a fabric do not show obvious change at the status of flat, folded (≈180°), or repetitive folding–unfolding cycles (20 cycles min^{-1}) (Figure 5b).

In summary, weavable hybrid fibers with sandwiched structure, i.e., MWCNT/rGO/MWCNT, have been successfully fabricated. Thus prepared fibers were then used as electrodes for solid-state supercapacitors. The supercapacitor based on MWCNT/rGO/MWCNT fibers with 90 wt% of GO loading exhibited excellent weavability, high energy density, good rate and cycling stability at high charge–discharge current density of 1.0 A cm^{-3} owing to the high electrical conductivity of well-aligned and long MWCNTs, the incorporation of rGO nanosheets, and the sandwiched hybrid structure of the MWCNT/rGO/MWCNT fiber. The novel unique structure, facile fabrication, and high performance of our fiber-based supercapacitors might provide promising application in the future e-textiles.

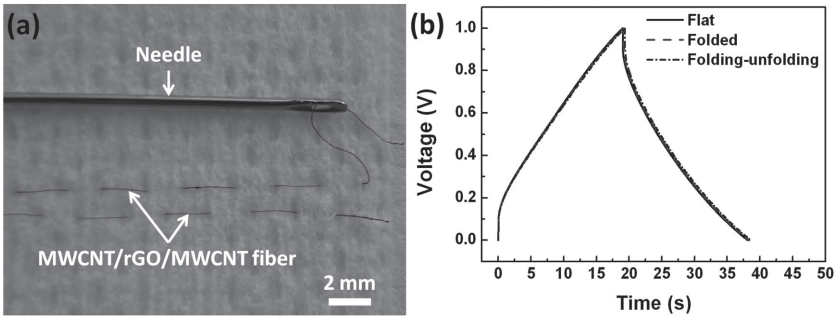

Figure 5. a) Photograph of two MWCNT/rGO/MWCNT fibers with 90 wt% of GO loading woven into a fabric by using a stainless steel needle. b) Galvanostatic charge–discharge curves (at current density of 1.0 A cm^{-3}) of a fiber-based supercapacitor woven into a fabric measured at the status of flat, folded (≈180°), or repetitive folding–unfolding cycles (20 cycles min^{-1}).

Experimental Section

As described in a previous work,[37] the growth of vertically aligned MWCNT array was achieved by chemical vapor deposition (CVD) in a quartz tube furnace at 750 °C for 10 min. Briefly, a 1 nm thick Fe film deposited on an Si/SiO_2 substrate was used as the catalyst. Ar (155 sccm) and C_2H_4 (45 sccm) were used as the carrier gas and carbon source, respectively. The well-aligned MWCNT sheet with areal density of ≈2.12 μg cm^{-2} was obtained by pulling the MWCNT array using a scotch tape. Graphene oxide (GO) nanosheets were prepared by a modified Hummer method,[38] which were then dispersed in DMF (99.8%, anhydrous, Sigma-Aldrich) with a concentration of 5 mg mL^{-1}.

Two layers of obtained MWCNT sheets with width of ≈1.5 mm and length of ≈8.5 cm were first stacked onto a PTFE substrate. The GO suspension was then drop-casted onto the MWCNT sheets, referred to as MWCNT/GO. Once it was dried, another two layers of MWCNT sheets were laid on top forming a sandwiched hybrid film, referred to as MWCNT/GO/MWCNT. Subsequently, this hybrid film was peeled off from the PTFE substrate and twisted into fiber with a motor rotating at 200 rpm for 2 min. The obtained MWCNT/GO/MWCNT fibers were immersed into HI (55 wt%, Sigma Aldrich, ACS reagent) at room temperature for 12 h to reduce GO in MWCNT/GO/MWCNT to form MWCNT/rGO/MWCNT.[29] For comparison, the MWCNT/rGO fiber was fabricated by twisting a MWCNT/GO hybrid film from the Step A in Figure 1a, followed by the aforementioned chemical reduction with HI. In addition, the rGO fiber was fabricated after the GO film was prepared by drop-casting a concentrated GO aqueous suspension of 20 mg mL^{-1} using the previously reported method,[39] followed by aforementioned chemical reduction with HI.

The solid-state fiber-based supercapacitors were fabricated and tested in two-electrode configuration similar to a previous study.[27] Briefly, two MWCNT/rGO/MWCNT fibers were placed closely and in parallel on a glass substrate, and then coated with PVA-H_2SO_4 gel electrolyte. The PVA-H_2SO_4 gel electrolyte was prepared by mixing H_2SO_4 (1 M, 10 mL) with PVA powder (1 g; M_W 85 000–124 000; Sigma Aldrich), followed by heating at 90 °C with vigorous stirring to obtain a homogeneous gel-like

suspension. Ag paste applied at both ends of the fibers served as the conductive pads for electrochemical measurements. The solid-state fiber-based supercapacitor woven into a fabric was prepared by sewing two MWCNT/rGO/MWCNT fibers (90 wt% of GO loading) into a fabric in parallel using a stainless steel needle (Figure 5a). After a layer of PVA-H_2SO_4 gel was coated on the fabric surface, the solid-state fiber-based supercapacitor was used for electrochemical tests.

The mechanical properties of fibers were measured using a precision micro-loading device (LCM SYSTEMS, UK), which is equipped with a screw displacement loading system and a micro-force measuring system with a maximum force of 25 gF and the precision of 0.01 gF.[40] The tensile tests were performed at a strain rate of 0.5 mm s^{-1} with a gauge length of 6 mm. The SEM images were obtained on a field-emission scanning electron microscope (JEOL, JSM-6700F, Japan). The electrical properties of fibers were characterized using semiconductor device parameter analyzer (Agilent Technologies B1500A, USA). XPS C1s spectra were recorded with AlKα radiation (1486.7 eV) using a VSW EA45 analyzer. The electrochemical measurements were obtained using a CHI 660D electrochemical work station. Atomic force microscopy (AFM, Cypher, Asylum Research, USA) was used to characterize the GO nanosheets in tapping mode in air.

The specific volumetric capacitance (C_V) of fiber-based supercapacitor was calculated from the galvanostatic charge–discharge curve according to the equation of $C_V = [i/(dV/dt)]/V_{fiber}$, where i is the discharge current, dV/dt is the slope of discharge curve, and V_{fiber} refers to the total volume of two fibers.

Supporting Information

Supporting Information is available from the Wiley Online Library or from the author.

Acknowledgements

This work was supported by the Singapore Ministry of Education under an AcRF Tier 2 grant (MOE2014-T2-1-003; ARC 26/13, No. MOE2013-T2-1-034; ARC 19/15, No. MOE2014-T2-2-093) and AcRF Tier 1 (RGT18/13, RG5/13), NTU under Start-Up Grant (M4081296.070.500000), NNSF of China (61328401), the Joint Research Fund for Overseas Chinese, Hong Kong and Macao Scholars (Grant No. 51528201), and Jiangsu Specially-Appointed Professor program (Grant No. 54935012). H. X. thanks the financial support from the National Natural Science Foundation of China (Grant No. GZ213054, 51322202) and the Natural Science Foundation of Jiangsu Province in China (Grant No. BK20130927).

Received: March 9, 2016
Revised: April 20, 2016
Published online:

[1] G. Z. Sun, X. W. Wang, P. Chen, *Mater. Today* **2015**, *18*, 215.
[2] X. F. Wang, B. Liu, R. Liu, Q. F. Wang, X. J. Hou, D. Chen, R. M. Wang, G. Z. Shen, *Angew. Chem., Int. Ed.* **2014**, *53*, 1849.
[3] B. Liu, D. S. Tan, X. F. Wang, D. Chen, G. Z. Shen, *Small* **2013**, *9*, 1998.
[4] H. H. Xu, X. L. Hu, Y. M. Sun, H. L. Yang, X. X. Liu, Y. H. Huang, *Nano Res.* **2015**, *8*, 1148.
[5] K. Jost, D. P. Durkin, L. M. Haverhals, E. K. Brown, M. Langenstein, H. C. De Long, P. C. Trulove, Y. Gogotsi, G. Dion, *Adv. Energy Mater.* **2015**, *5*, 1401286.
[6] Y. P. Fu, X. Cai, H. W. Wu, Z. B. Lv, S. C. Hou, M. Peng, X. Yu, D. C. Zou, *Adv. Mater.* **2012**, *24*, 5713.
[7] D. S. Yu, S. L. Zhai, W. C. Jiang, K. L. Goh, L. Wei, X. D. Chen, R. R. Jiang, Y. Chen, *Adv. Mater.* **2015**, *27*, 4895.
[8] G. Z. Sun, J. Q. Liu, X. Zhang, X. W. Wang, H. Li, Y. Yu, W. Huang, H. Zhang, P. Chen, *Angew. Chem., Int. Ed.* **2014**, *53*, 12576.
[9] C. S. Xiang, C. C. Young, X. Wang, Z. Yan, C. C. Hwang, G. Cerioti, J. Lin, J. Kono, M. Pasquali, J. M. Tour, *Adv. Mater.* **2013**, *25*, 4592.
[10] Z. Xu, H. Y. Sun, X. L. Zhao, C. Gao, *Adv. Mater.* **2013**, *25*, 188.
[11] R. Jalili, S. H. Aboutalebi, D. Esrafilzadeh, R. L. Shepherd, J. Chen, S. Aminorroaya-Yamini, K. Konstantinov, A. I. Minett, J. M. Razal, G. G. Wallace, *Adv. Funct. Mater.* **2013**, *23*, 5345.
[12] H. P. Cong, X. C. Ren, P. Wang, S. H. Yu, *Sci. Rep.* **2012**, *2*, 613.
[13] Z. L. Dong, C. C. Jiang, H. H. Cheng, Y. Zhao, G. Q. Shi, L. Jiang, L. T. Qu, *Adv. Mater.* **2012**, *24*, 1856.
[14] B. Xu, S. F. Yue, Z. Y. Sui, X. T. Zhang, S. S. Hou, G. P. Cao, Y. S. Yang, *Energy Environ. Sci.* **2011**, *4*, 2826.
[15] L. Kou, T. Huang, B. Zheng, Y. Han, X. Zhao, K. Gopalsamy, H. Y. Sun, C. Gao, *Nat. Commun.* **2014**, *5*, 3754.
[16] G. Z. Sun, J. Q. Liu, L. X. Zheng, W. Huang, H. Zhang, *Angew. Chem., Int. Ed.* **2013**, *52*, 13351.
[17] G. Z. Sun, Y. N. Zhang, L. X. Zheng, *J. Nanomater.* **2012**, *2012*, 506209.
[18] X. B. Zhang, K. L. Jiang, C. Teng, P. Liu, L. Zhang, J. Kong, T. H. Zhang, Q. Q. Li, S. S. Fan, *Adv. Mater.* **2006**, *18*, 1505.
[19] M. Zhang, K. R. Atkinson, R. H. Baughman, *Science* **2004**, *306*, 1358.
[20] N. Behabtu, M. J. Green, M. Pasquali, *Nano Today* **2008**, *3*, 24.
[21] S. Ilani, L. A. K. Donev, M. Kindermann, P. L. McEuen, *Nat. Phys.* **2006**, *2*, 687.
[22] D. Yu, K. Goh, H. Wang, L. Wei, W. Jiang, Q. Zhang, L. M. Dai, Y. Chen, *Nat. Nanotechnol.* **2014**, *9*, 555.
[23] Y. W. Ma, P. Li, J. W. Sedloff, X. Zhang, H. B. Zhang, J. Liu, *ACS Nano* **2015**, *9*, 1352.
[24] F. Tristan-Lopez, A. Morelos-Gomez, S. M. Vega-Diaz, M. L. Garcia-Betancourt, N. Perea-Lopez, A. L. Elias, H. Muramatsu, R. Cruz-Silva, S. Tsuruoka, Y. A. Kim, T. Hayahsi, K. Kaneko, M. Endo, M. Terrones, *ACS Nano* **2013**, *7*, 10788.
[25] N. Jung, S. Kwon, D. Lee, D. M. Yoon, Y. M. Park, A. Benayad, J. Y. Choi, J. S. Park, *Adv. Mater.* **2013**, *25*, 6854.
[26] M. K. Shin, B. Lee, S. H. Kim, J. A. Lee, G. M. Spinks, S. Gambhir, G. G. Wallace, M. E. Kozlov, R. H. Baughman, S. J. Kim, *Nat. Commun.* **2012**, *3*, 650.
[27] G. Z. Sun, X. Zhang, R. Z. Lin, J. Yang, H. Zhang, P. Chen, *Angew. Chem., Int. Ed.* **2015**, *54*, 4651.
[28] M. D. Lima, S. L. Fang, X. Lepro, C. Lewis, R. Ovalle-Robles, J. Carretero-Gonzalez, E. Castillo-Martinez, M. E. Kozlov, J. Y. Oh, N. Rawat, C. S. Haines, M. H. Haque, V. Aare, S. Stoughton, A. A. Zakhidov, R. H. Baughman, *Science* **2011**, *331*, 51.
[29] I. K. Moon, J. Lee, R. S. Ruoff, H. Lee, *Nat. Commun.* **2010**, *1*, 73.
[30] U. N. Maiti, J. Lim, K. E. Lee, W. J. Lee, S. O. Kim, *Adv. Mater.* **2014**, *26*, 615.
[31] K. Naoi, P. Simon, *J. Electrochem. Soc.* **2008**, *17*, 34.
[32] Y. Chen, X. O. Zhang, D. C. Zhang, P. Yu, Y. W. Ma, *Carbon* **2011**, *49*, 573.
[33] X. Xiao, T. Q. Li, P. H. Yang, Y. Gao, H. Y. Jin, W. J. Ni, W. H. Zhan, X. H. Zhang, Y. Z. Cao, J. W. Zhong, L. Gong, W. C. Yen, W. J. Mai, J. Chen, K. F. Huo, Y. L. Chueh, Z. L. Wang, J. Zhou, *ACS Nano* **2012**, *6*, 9200.
[34] P. Xu, T. L. Gu, Z. Y. Cao, B. Q. Wei, J. Y. Yu, F. X. Li, J. H. Byun, W. N. Lu, Q. W. Li, T. W. Chou, *Adv. Energy Mater.* **2014**, *4*, 1300759.
[35] C. Choi, J. A. Lee, A. Y. Choi, Y. T. Kim, X. Lepro, M. D. Lima, R. H. Baughman, S. J. Kim, *Adv. Mater.* **2014**, *26*, 2059.
[36] B. S. Shim, W. Chen, C. Doty, C. L. Xu, N. A. Kotov, *Nano Lett.* **2008**, *8*, 4151.
[37] G. Z. Sun, J. Y. Zhou, F. Yu, Y. N. Zhang, J. H. L. Pang, L. X. Zheng, *J. Solid State Electrochem.* **2012**, *16*, 1775.
[38] X. Z. Zhou, X. Huang, X. Y. Qi, S. X. Wu, C. Xue, F. Y. C. Boey, Q. Y. Yan, P. Chen, H. Zhang, *J. Phys. Chem. C* **2009**, *113*, 10842.
[39] R. Cruz-Silva, A. Morelos-Gomez, H. I. Kim, H. K. Jang, F. Tristan, S. Vega-Diaz, L. P. Rajukumar, A. L. Elias, N. Perea-Lopez, J. Suhr, M. Endo, M. Terrones, *ACS Nano* **2014**, *8*, 5959.
[40] Y. N. Zhang, L. X. Zheng, G. Z. Sun, Z. Y. Zhan, K. Liao, *Carbon* **2012**, *50*, 2887.

